



Analysis of pyrolysis products from light hydrocarbons and kinetic modeling for growth of polycyclic aromatic hydrocarbons with detailed chemistry

Koyo Norinaga^{a,b,c,*}, Olaf Deutschmann^b, Naomichi Saegusa^a, Jun-ichiro Hayashi^{a,c}

^a Center for Advanced Research of Energy Conversion Materials, Hokkaido University, N13-W8, Kitaku, Sapporo 060-8628, Japan

^b Institut für Technische Chemie und Polymerchemie, Universität Karlsruhe, Engesserstr. 20, 76131 Karlsruhe, Germany

^c Institute for Materials Chemistry and Engineering, Kyushu University, Kasuga, Fukuoka 816-8580, Japan

ARTICLE INFO

Article history:

Received 18 July 2008

Accepted 12 May 2009

Available online 21 May 2009

Keywords:

Polycyclic aromatic hydrocarbon

Light hydrocarbon

Carbon deposition

Chemical reaction kinetics

Modeling

ABSTRACT

Alternative chemical reaction pathways leading to polycyclic aromatic hydrocarbons (PAHs) in the pyrolysis of unsaturated light hydrocarbons were investigated to extend the previously proposed chemical kinetic model [K. Norinaga, O. Deutschmann, *Ind. Eng. Chem. Res.* 46 (2007) 3547–3557]. Although the previous model provided a reasonably good description of the pyrolysis behaviors observed in flow reactor experiments at 1073–1373 K, the concentration profiles for large PAHs were underestimated significantly. In this study, pyrolysates from ethylene, acetylene, and propylene were analyzed in detail using gas chromatography/mass spectroscopy (GC/MS) to find the intermediates that are believed to be crucial for PAH formation. Based on the newly identified products, reaction schemes for aromatic growth via 1,2-diphenylethylene, 1,2-diphenylacetylene, triphenylene, and benz[*f*]indene were proposed and added to the previous model. The predictive capabilities improved slightly simply because of the minority of the newly found compounds. The addition of reaction schemes for self-combination of indenyl radicals to form benz[*a*]anthracene and chrysene had a significant effect, and were found to be necessary to account for the formation of large PAHs such as benz[*a*]anthracene, chrysene, and benz[*a*]pyrene. Results from reaction flux analysis to identify the likely chemical pathways important for PAH growth, as well as numerical simulations of the influence of acetone contamination on acetylene pyrolysis, are presented.

© 2009 Elsevier B.V. All rights reserved.

1. Introduction

Pyrolytic carbon formed during hydrocarbon pyrolysis by chemical vapor deposition (CVD) is a material that is used in a variety of applications from coatings of nuclear reactor fuel particles to aircraft disk brakes [1]. The CVD of carbon implies that the precursor hydrocarbon, which is often methane [2–4], propane [5–7], or sometimes unsaturated hydrocarbons such as propylene [8,9] and ethylene [10–12], is heated to the deposition temperature, resulting in complex gas-phase reactions (homogeneous pyrolysis reactions) that are competing or interacting with complex surface reactions (heterogeneous deposition reactions). Gas-phase reactions of light hydrocarbons are synthesis reactions in which a wide variety of molecules and radicals, from the smallest species of hydrogen radical to larger species of polycyclic aromatic hydrocarbon (PAH), are formed. Carbon deposition is also

an important issue in industrial technologies of hydrocarbon processing, such as cracking of light alkanes [13]. Understanding the chemistry and kinetics of gas-phase reactions is essential to expanding our knowledge of the carbon deposition mechanism [14]. Yet, the precise mechanism of hydrocarbon pyrolysis, including formations of minor products such as PAHs, is not well understood.

A detailed chemical kinetic approach to develop a reaction mechanism consisting of hundreds or thousands of elementary-like reaction steps is a promising method for elucidating an accurate description of the phenomena that occur in the gas phase. Several detailed kinetic models for the pyrolysis of light hydrocarbons including methane [15], ethylene [16], acetylene [16], propane [17–19], propylene [16], and butane [20], have been proposed. However, successful modeling of the gas-phase reactions involving an aromatic growth mechanism using elementary reactions is extremely difficult due to the high branching ratio in the PAH formations. We developed a detailed gas-phase reaction mechanism for the pyrolysis of ethylene, acetylene, and propylene [16] that encompasses the formation of PAHs up to coronene. Comparisons were made between experiments and computations for more than 30 compounds, including hydrogen and hydro-

* Corresponding author at: Institute for Materials Chemistry and Engineering, Kyushu University, Kasuga, Fukuoka 816-8580, Japan. Tel.: +81 92 583 7793; fax: +81 92 583 7796.

E-mail address: norinaga@cm.kyushu-u.ac.jp (K. Norinaga).

carbons ranging from methane to coronene. These demonstrated that the mechanism has a comprehensive capability for predicting concentration profiles of the major components (mole fractions larger than 10^{-2}) found in the pyrolysis of three different hydrocarbons at 1173 K with an acceptable level of accuracy. Although disagreements were observed for minor species, especially for PAHs for which the formations were appreciably underestimated. In addition, we extended model validations at varying temperatures, ranging from 1073 to 1373 K [21]. The model could predict the profiles of major products in the pyrolysis of three hydrocarbons with satisfactory accuracy over the whole temperature range. Mole fraction profiles of minor compounds, including PAHs up to phenanthrene and anthracene, were also modeled fairly well. Appreciable underestimates, by one to four orders of magnitude, were observed for the larger PAHs at temperatures below 1273 K, where the deviation increases with decreasing temperature and increasing molecular mass of PAHs. Better agreements were found at temperatures above 1323 K. Reasons attributing to the gaps found in the PAH concentrations are likely to include a lack of chemistry for the PAH formation, inadequate kinetic parameters for reactions that are sensitive to PAH concentrations at lower temperatures, ignorance of the diffusion of species, as well as surface reactions.

In this study, possible pathways leading to the PAHs that were not considered in our previous chemical kinetic model [16] were examined to enhance the predictive capabilities of PAH concentration profiles. Three light hydrocarbons, including ethylene, acetylene, and propylene, were pyrolyzed at conditions relevant to the CVD of carbon, and the pyrolysates were analyzed in detail using gas chromatography/mass spectroscopy (GC/MS) to find the compounds crucial to PAH formation. Based on these newly found products, possible reaction pathways were proposed and added to our reaction mechanism for hydrocarbon pyrolysis. The kinetic parameters of these reactions were estimated from those for analogous reactions for which rate constants are known. Finally, the proposed reaction mechanism was crucially evaluated by carrying out comparisons between experimental data and the predictions from numerical simulations.

2. Experimental

The experimental setup is shown in Fig. 1. A vertical flow reactor with a total length 0.44 m was used to pyrolyze ethylene,

acetylene, and propylene at a total pressure of 8 kPa over a temperature range of 1073–1373 K with 50 K increments with no diluent gas. Temperature profiles along the reactor wall were also given. The flow rate of inlet source gas was controlled such that the space time at the isothermal zone was fixed at 0.5 s.

The products were analyzed quantitatively using both on-line and off-line gas chromatography. A detailed description of the experimental setup and product analysis was reported previously [22]. Additionally, detailed qualitative analyses of the condensing products larger than benzene were performed using GC/MS. The condensing products were collected in two cold traps set at 195 K and recovered by solvent extraction with acetone. The acetone extract was analyzed with a GC/MS system consisting of a Shimadzu GC-17A gas chromatograph coupled to a Shimadzu QP-5000 mass spectrometer at an ionization energy of 70 eV in the electron impact mode with a scan range of 50–300 m/z . The GC column was a TC-5 (30 m \times 0.25 mm, film thickness: 0.25 μm , GL Science Co.), which has a stationary phase of cross-linked 5% diphenyl-95% dimethylpolysiloxane. The product solution (1.0 μl) was injected into the gas chromatograph under splitless conditions, with the temperature program consisting of 5 min at 313 K, followed by an increase to 573 K at a rate of 4 K min^{-1} , followed by 30 min at 573 K. Peaks were identified by matching the retention time and using a mass spectral library attached to the Shimadzu MS workstation CLASS-5000.

3. Experimental results

The total ion chromatogram from the GC/MS analysis of the condensing products from ethylene pyrolysis at 1273 K is shown in Fig. 2. The condensing products from ethylene and acetylene were qualitatively similar in that they contained almost the same set of identified components (see Supporting Information). The condensing products were resolved to more than 80 peaks, of which approximately 50 were identified. The boxed compounds (such as 1-propynylbenzene, indane, triphenylene, 1-methyleneindene, biphenylene, 2-vinylnaphthalene, 1-vinylnaphthalene, acenaphthene, 1H-phenalene, 1-methylacenaphthylene, benz[f]indene, diphenylethylene, diphenylacetylene, 4-methylpyrene, triphenylene) were not identified in the previous GC study of pyrolysates from methane [23], ethylene, acetylene, and propylene [22]. Biphenylene, 2-vinylnaphthalene, and 1-vinylnaphthalene were already involved in the reaction mechanism [16], but the other newly identified compounds were not.

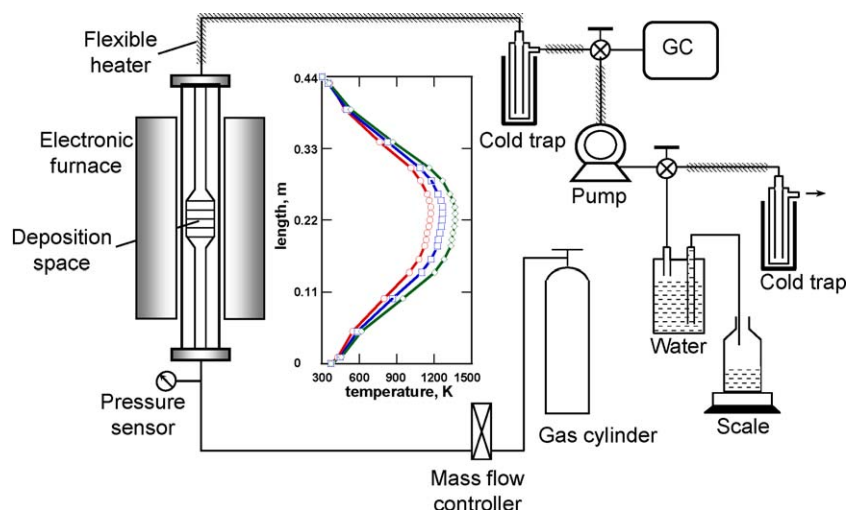


Fig. 1. Experimental setup for studying product distributions in CVD of carbon and experimentally obtained temperature profiles along the reactor wall. Temperatures of the quasi-isothermal zones are (from left to right) 1173, 1273, and 1373 K. The wall temperature profiles are approximated by connecting measured points with linear lines for use in the DETCHEM^{PLUG} simulations.

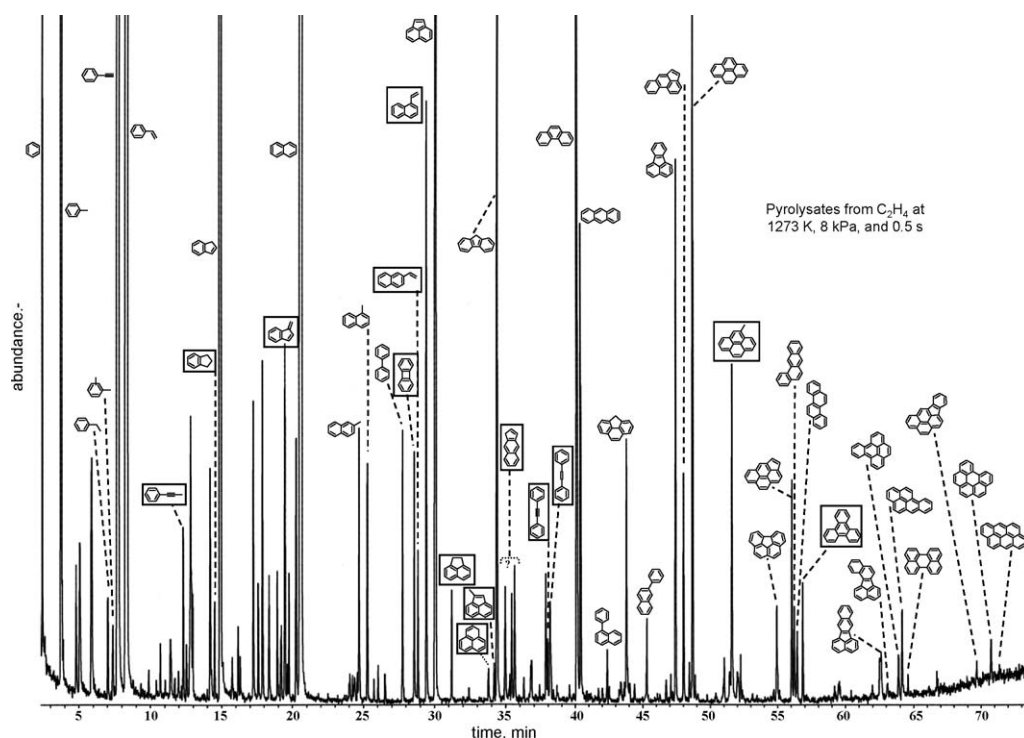


Fig. 2. Total ion chromatogram from GC/MS analysis of the condensing products from the pyrolysis of ethylene at 1273 K, 8 kPa, and a residence time of 0.5 s in a tubular flow reactor. Identified compounds (from left to right) are benzene, toluene, ethylbenzene, xylene, phenylacetylene, styrene, 1-propynylbenzene, indane, indene, 1-methyleneindene, naphthalene, 2-methylnaphthalene, 1-methylnaphthalene, biphenyl, biphenylene, 2-vinylnaphthalene, 1-vinylnaphthalene, acenaphthylene, acenaphthene, 1H-phenalene, 1-methylacenaphthylene, fluorene, benz[f]indene, diphenylethylene, diphenylacetylene, phenanthrene, anthracene, 1-phenylnaphthalene, 4H-cyclopenta[def]phenanthrene, 2-phenylnaphthalene, fluoranthene, acephenanthrylene, pyrene, 4-methylpyrene, benzo[ghi]fluoranthene, cyclopenta[cd]pyrene, benz[a]anthracene, chrysene, triphenylene, benzo[k]fluoranthene, benzo[j]fluoranthene, benzo[e]pyrene, benzo[a]pyrene, perylene, o-phenylene-pyrene, benzo[ghi]perylene, and bibenzo[def,mno]chrysene. Boxed compounds indicate compounds that were not involved in the original reaction mechanism of Ref. [16].

The identification of benz[f]indene, however, has controversy. The mass spectrum of the three peaks that eluted after fluorene (elution time 35–36 min) indicated that the mass numbers of the precursor ions are 166 m/z , suggesting that the elution of fluorene isomers ($C_{13}H_{10}$) contributes to these peaks. The possible $C_{13}H_{10}$ isomers are 1-methylbiphenylene, 2-methylbiphenylene, benz[f]indene, benz[e]indene, and so on. Wornat et al. first identified benz[f]indene among the pyrolysis products of anthracene using high-pressure liquid chromatography with diode-array ultraviolet–visible detection [24]. They also found benz[f]indene in the pyrolysis products of catechol [25]. Although we are currently unable to identify these peaks because of commercial inavailability and lack of mass spectrum data of this compound, it is not daring to assign benz[f]indene to one of these undefined peaks and to assert its presence in the products of the light hydrocarbon pyrolysis based on the evidences that the precursor ion mass number is 166 m/z and the findings of Wornat et al. [24,25].

In the following, the mechanism [16] is updated by incorporating the newly identified compounds in order to improve the predictability of the PAH profiles which were appreciably underestimated.

4. Modeling

The original mechanism [16] consisted of 227 species and 827 elementary step-like reactions, of which 798 were reversible. The mechanism and thermodynamic data for all species may be downloaded (www.detchem.com).

Calculations were performed using the gas-phase reaction mechanism with the PLUG code in the DETCHEM program package (DETCHEM^{PLUG}). DETCHEM^{PLUG} is designed for the non-dispersive one-dimensional flow of chemically reacting ideal gas mixtures

under steady state conditions. The system of differential algebraic equations (DAE) describing the plug flow reactor consisted of the continuity equation, species conservation equation, energy equation, and the equation of state. The system of equations was solved using the differential algebraic equation solver LIMEX.

The input parameters for the simulations were obtained from the experimental conditions, including the wall temperature profiles, inlet velocity, molar composition, and pressure. The purity of the source hydrocarbons and the initial compositions used in the computations are given in Table 1. The composition of the source hydrocarbons was based on values reported by the supplier, with the exception of acetylene, which was analyzed by GC/MS and found to contain 2% (v/v) acetone. Since acetylene is dissolved in acetone for transport and storage to prevent explosion, the high fraction of acetone was not surprising. In the computations for acetylene pyrolysis, the initial acetone volume fraction was fixed at 0.018, although the acetone concentration depends on the total pressure of acetylene bottle as discussed by Bergmann et al. [26]. Computations were performed for seven different temperature profiles with the temperature in the quasi-isothermal zone ranging from 1073–1373 K. A detailed description of the numerical simulation with DETCHEM^{PLUG} is given elsewhere [21].

Table 1

Properties of the source gases and the initial compositions used in the computations.

Source hydrocarbons	Purity (vol%) ^a	Composition used in the computation (mole fractions, –)
Ethylene	>99.4	C_2H_4 0.994, CH_4 0.002, C_2H_6 0.004
Acetylene	>99.6	C_2H_2 0.980, CH_4 0.002, acetone 0.018
Propylene	>99.5	C_3H_6 0.996, CH_4 0.001, C_3H_8 0.003

^a Values reported by the supplier (Air Liquide Co.).

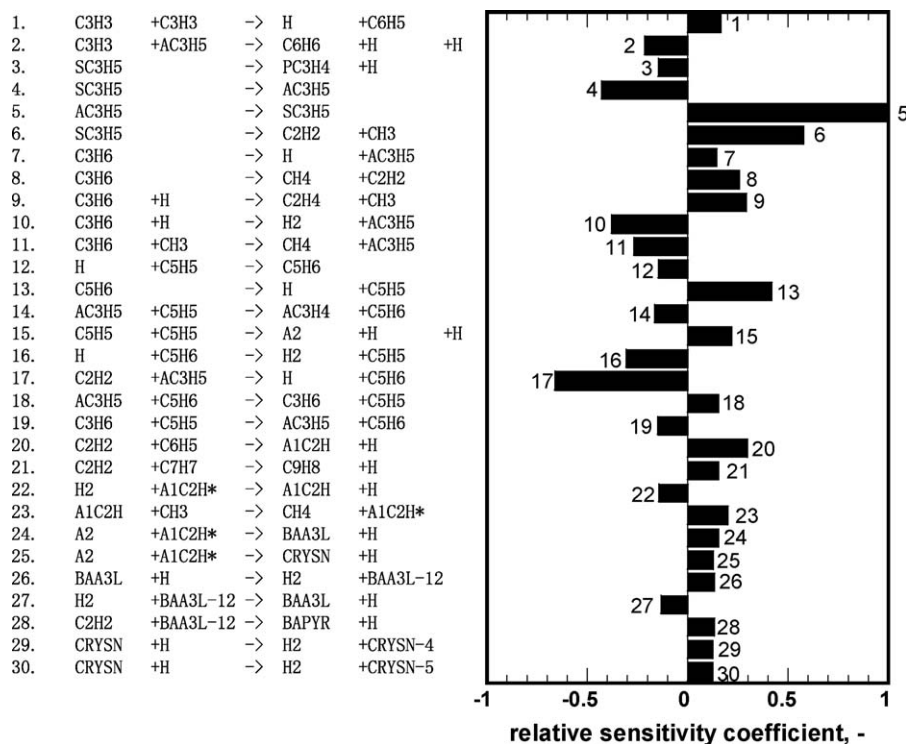


Fig. 3. Sensitivity analysis for benzo[a]pyrene in pyrolysis of propylene at 1173 K, 8 kPa, and a residence time of 0.5 s.

Sensitivity and reaction flux analyses were also performed using the HOMREA software package [27].

5. Modeling results and discussion

5.1. First attempt: PAH radical formations by methyl and vinyl radical attacks

Prior to adding new reactions that lead to PAHs, a sensitivity analysis was performed on the original reaction mechanism [16] to identify the reactions that are crucial to the formation of large

PAHs. Shown in Fig. 3 are the results from the sensitivity analysis with respect to benzo[a]pyrene, which was chosen as an example since its concentration was significantly underestimated at lower temperatures. Several reactions were identified that may influence the formation of benzo[a]pyrene. The isomerization of the allyl radical to a 1-propenyl radical (No. 5) was the most sensitive reaction for benzo[a]pyrene formation. This means that the predicted concentration of benzo[a]pyrene was influenced most by a change in the rate of this reaction. Although modification of the rate parameter for this reaction should be the most effective method for bringing the predicted value closer to the actual

Table 2

Additions and modifications to the reaction mechanism reported by Norinaga and Deutschmann [16]. $k = AT^n \exp(-E_a/RT)$.

No. ^a	Reaction ^b	A (mol, cm ³ , s)	n	E _a (kJ/mol)	No of analogous reactions or comments
Additions by Attempt 1					
<i>Methyl radical attack</i>					
828.	A3 +CH3 =A3-4 +CH4	2.00E+12	0.0	63.0	577
829.	BAA3L +CH3 =BAA3L-1 +CH4	2.00E+12	0.0	63.0	577
830.	BAA3L +CH3 =BAA3L-12 +CH4	2.00E+12	0.0	63.0	577
831.	CRYSN +CH3 =CRYSN-4 +CH4	2.00E+12	0.0	63.0	577
832.	CRYSN +CH3 =CRYSN-5 +CH4	2.00E+12	0.0	63.0	577
833.	PERYLN +CH3 =PERYLN* +CH4	2.00E+12	0.0	63.0	577
834.	BEPYR +CH3 =BEPYR* +CH4	2.00E+12	0.0	63.0	577
835.	BEPYR +CH3 =BEPYR-2 +CH4	2.00E+12	0.0	63.0	577
836.	BAPYR +CH3 =BAPYR* +CH4	2.00E+12	0.0	63.0	577
837.	BAPYR +CH3 =BAPYR-2 +CH4	2.00E+12	0.0	63.0	577
838.	BGHIPE +CH3 =BGHIPE* +CH4	2.00E+12	0.0	63.0	577
<i>Vinyl radical attack</i>					
839.	A2 +C2H3 =A2-1 +C2H4	6.00E+11	0.0	54.3	472
840.	A2 +C2H3 =A2-2 +C2H4	6.00E+11	0.0	54.3	472
841.	A3 +C2H3 =A3-4 +C2H4	6.00E+11	0.0	54.3	472
842.	BAA3L +C2H3 =BAA3L-1 +C2H4	6.00E+11	0.0	54.3	472
843.	BAA3L +C2H3 =BAA3L-12 +C2H4	6.00E+11	0.0	54.3	472
844.	CRYSN +C2H3 =CRYSN-4 +C2H4	6.00E+11	0.0	54.3	472
845.	CRYSN +C2H3 =CRYSN-5 +C2H4	6.00E+11	0.0	54.3	472
846.	PERYLN +C2H3 =PERYLN* +C2H4	6.00E+11	0.0	54.3	472
847.	BEPYR +C2H3 =BEPYR* +C2H4	6.00E+11	0.0	54.3	472
848.	BEPYR +C2H3 =BEPYR-2 +C2H4	6.00E+11	0.0	54.3	472

Table 2 (Continued)

No. ^a	Reaction ^b	A(mol, cm ³ , s)	n	E _a (kJ/mol)	No of analogous reactions or comments
849.	BAPYR +C2H3 =BAPYR* +C2H4	6.00E+11	0.0	54.3	472
850.	BAPYR +C2H3 =BAPYR-2 +C2H4	6.00E+11	0.0	54.3	472
851.	BGHIPE +C2H3 =BGHIPE* +C2H4	6.00E+11	0.0	54.3	472
Etc.					
852.	BEPYR +H =BEPYR-2 +H2	3.23E+07	2.1	66.3	812
853.	BAPYR +H =BAPYR-2 +H2	3.23E+07	2.1	66.3	812
854.	BEPYR-2 +H =BEPYR	5.00E+13	0.0	0.0	813
855.	BAPYR-2 +H =BAPYR	5.00E+13	0.0	0.0	813
856.	BEPYR-2 +C2H2 =BGHIPE +H	1.87E+07	1.8	13.7	817
857.	BAPYR-2 +C2H2 =ANTHAN +H	1.87E+07	1.8	13.7	817
Additions by Attempt 2					
<i>Triphenylene route</i>					
858.	P2- +C6H5 =P3	5.94E+42	-8.8	57.9	458
859.	P2- +C6H5 =P3- +H	8.60E+13	0.5	145.7	459
860.	P2 +C6H5 =P3 +H	9.50E+75	-18.9	165.2	476
861.	P2- +C6H6 =P3 +H	9.50E+75	-18.9	165.2	476
862.	P2- +C6H6 =A4T +H2 +H	8.51E+11	0.0	16.7	700
863.	P2 +C6H5 =A4T +H2 +H	8.51E+11	0.0	16.7	700
864.	P2- +C6H5 =A4T +H +H	1.39E+13	0.0	0.46	602
865.	P3 +H =P3- +H2	3.23E+07	2.1	66.3	678
866.	P3- +H =P3	1.17E+33	-5.6	36.7	679
867.	P3- =A4T +H	9.50E+75	-18.9	165.2	476
868.	A4T +CH3 =A4T- +CH4	2.00E+12	0.0	62.7	469
869.	P3 +CH3 =P3- +CH4	2.00E+12	0.0	62.7	469
870.	A4T +C2H3 =A4T- +C2H4	6.00E+11	0.0	54.3	472
871.	P3 +C2H3 =P3- +C2H4	6.00E+11	0.0	54.3	472
872.	A4T- +H =A4T	5.00E+13	0.0	0.0	813
873.	A4T- +C2H2 =BEPYR +H	1.87E+07	1.8	13.7	699
874.	A4T +H =A4T- +H2	3.23E+07	2.1	66.3	812
<i>1,2-Diphenylethane, 1,2-diphenylethene, 1,2-diphenylethyne routes</i>					
875.	C7H7 +C7H7 =BBNZYL	1.15E+13	0.0	0.0	^c
876.	C7H8 +C7H7 =BBNZYL +H	1.20E+12	0.0	66.7	516
877.	BBNZYL +H =BBNZYL- +H2	3.23E+07	2.1	66.3	682
878.	BBNZYL +CH3 =BBNZYL- +CH4	2.00E+12	0.0	62.7	469
879.	BBNZYL +C2H3 =BBNZYL- +C2H4	6.00E+11	0.0	54.3	472
880.	BBNZYL- +H =A3H2	4.00E+11	0.0	50.2	681
881.	A3H2 +H =HA3 +H2	5.40E+02	3.5	21.8	676
882.	A3H2 =A3 +H2	4.70E+13	0.0	257.8	677
883.	HA3 +H =A3 +H2	1.81E+12	0.0	0.0	674
884.	HA3 +H =A3H2	1.00E+14	0.0	0.0	675
885.	A1C2H3 +C6H5 =DPETE +H	2.50E+12	0.0	25.9	450
886.	N-A1C2H2 +C6H5 =DPETE	3.90E+38	-7.6	54.0	447
887.	N-A1C2H2 +C6H6 =DPETE +H	0.80E+12	0.0	26.8	471
888.	DPETE +H =DPETE* +H2	2.19E+08	1.8	12.6	558
889.	DPETE +CH3 =DPETE* +CH4	3.10E+11	0.0	23.0	559
890.	DPETE +C2H3 =DPETE* +C2H4	4.40E+00	3.5	17.1	560
891.	DPETE* =A3 +H	4.00E+11	0.0	50.2	681
892.	DPETE* +H =DPETE	1.17E+33	-5.6	36.7	679
Additions by Attempt 3					
893.	C9H7 +C9H7 =CRYSN +H +H	1.00E+12	0.0	33.5	Estimated ^d
894.	C9H7 +C9H7 =BAA3L +H +H	1.00E+12	0.0	33.5	Estimated ^d
895.	C9H7 +C2H2 =A2CH2-2	5.00E+11	0.0	43.3	508 ^e
896.	A2CH2-2 +C2H2 =BFinden +H	1.00E+11	0.0	29.3	513
897.	A2C2H2-2 +CH3 =BFinden +H +H	5.00E+13	0.0	0.0	543
898.	BFinden +H =BFinden- +H2	2.19E+08	1.8	12.6	558
899.	BFinden +CH3 =BFinden- +CH4	3.10E+11	0.0	23.0	559
900.	BFinden +C2H3 =BFinden- +C2H4	4.40E+00	3.5	17.1	560
901.	BFinden- +C5H5 =BAA3L +H +H	1.00E+12	0.0	33.5	Estimated ^d
902.	BFinden- +H =BFinden	2.00E+14	0.0	0.0	555
Modifications by Attempt 3					
395.	C5H5 +C5H5 =A2 +H +H	2.00E+13	0.0	33.5	^f
557.	C9H7 +C5H5 =A3 +H +H	1.00E+13	0.0	33.5	^f

^a Numbering starts from 828 because the reaction mechanism from Ref. [16] involved 827 reactions.

^b The species nomenclature is the same as reported previously [16], also given in the Supporting Information. For example, A3 denotes phenanthrene, BAA3L benzo[a]anthracene, CRYSN chrysene, PERYLN perylene, BEPYR benzo[e]pyrene, BAPYR benzo[a]pyrene, BGHIPE benzo[ghi]perylene, A2 naphthalene, ANTHAN anthanthracene, P2 biphenyl, P3 terphenyl, A4T triphenylene, BBNZYL bibenzyl, A3H2 dihydrophenanthrene, A1C2H3 styrene, N-A1C2H2 styryl radical, DPETE diphenylethylene, A2C2H-1 1-ethynylphenanthrene, C9H7 indenyl radical, A3CH2R cyclopenta[def]phenanthrene, and BFinden benz[fi]ndene.

^c Estimated with RMG [32–35].

^d $k_{557} \times 0.1$.

^e Estimated from the reverse of reaction 508.

^f Ref. [36].

measurement, changing this parameter also influences the accuracy of predicting the formation/consumption profiles of major products such as hydrogen, methane, ethylene, propyne, benzene, and propylene. Since the accuracy of predicting the concentration profiles of major species was excellent [16,21], any change in the rate parameter for this reaction was undesirable from the viewpoint of maintaining the entire performance of this kinetic model. Thus, we subsequently examined reactions that had little influence on the concentration of major species, but exhibited sensitivity in benzo[a]pyrene formation. These included H-abstraction from benz[a]anthracene and chrysene by H radical attack (reaction Nos. 26, 29, and 30). Benzo[a]pyrene was then generated by the addition of acetylene to the PAH radicals formed by these reactions according to the hydrogen abstraction acetylene addition (HACA) mechanism [28,29].

To promote the PAH radical generation, PAH radicals formed by reactive radicals such as methyl and vinyl radicals were also considered in addition to those formed by H attack. The H-abstractions from aromatic hydrocarbons by methyl and vinyl radicals were also proposed by Ziegler et al. [19]. Relevant elementary step-like reactions are given in Table 2 (Attempt 1). The effects of these modifications on the simulation results for typical PAHs in propylene pyrolysis at 1173 K are shown in Table 3. The effects were very small, except for pyrene and benzo[a]pyrene, for which concentrations were increased from the original predictions by five- and two-fold, respectively. Enhanced formation of phenanthryl radical as well as radicals of chrysene and benz[a]anthracene, which are precursors of pyrene and benzo[a]pyrene, respectively, were partly responsible for these increments. The predicted mole fractions of pyrene and benzo[a]pyrene were still smaller than the measured values by one and four orders of magnitude, respectively. The small or negligible effects at 1173 K were likely attributable to the small concentrations of methyl and vinyl radicals as well as the low rate of hydrogen abstractions from PAHs by these radicals due to the high activation energies of the reactions.

5.2. Second attempt: aromatic growth pathways through 1,2-diphenylethylene, 1,2-diphenylacetylene, and triphenylene

The 1,2-diphenylethylene and 1,2-diphenylacetylene were newly identified compounds. The reaction pathways through these compounds (shown in Fig. 4) were proposed by Bruinsma and Moulijn [30]. Triphenylene was also newly found, and an aromatic growth route through this compound proposed by Dong and Hüttinger [23] is also shown. Based on these reaction schemes, a mechanism consisting of elementary step-like reactions was developed, as listed in Table 2 (Attempt 2). The kinetic parameters for the reactions were estimated based on their analogous reactions. The thermodynamic data for several compounds that were not available from the literature were estimated based on the Benson's group additivity method [31] using software developed by Green et al. (RMG) [32–35]. Results from numerical simulations of adding the reactions derived from both the first and second attempts are given in Table 3. The second attempt had almost no effect on the predicted mole fractions of the typical PAHs, and underestimations by one to four orders of magnitude remained for the PAHs, except for phenanthrene. The predicted mole fractions of 1,2-diphenylethylene and 1,2-diphenylacetylene were in the range of 10^{-5} in the propylene pyrolysis at 1173 K. While 1,2-diphenylethylene and 1,2-diphenylacetylene were found experimentally, they are products of minor importance in the formation of phenanthrene. The predicted mole fraction of triphenylene was as small as 10^{-6} in the propylene pyrolysis at 1173 K, also making it an insignificant precursor of benz[e]pyrene.

Table 3
Experimentally measured and numerically predicted concentrations of typical PAHs found in propylene pyrolysis at 1173 K, 8 kPa, and a residence time of 0.5 s in a flow reactor.

Measured mole fraction, –	Phenanthrene 5.6E-04		Pyrene 2.0E-04		Benzo[a]anthracene 2.4E-05		Chrysen 5.6E-05		5 Benzo[a]pyrene 1.5E-0		Benzo[e]pyrene 2.1E-05	
	Predicted mole fraction, –	Ratio, –	Predicted mole fraction, –	Ratio, –	Predicted mole fraction, –	Ratio, –	Predicted mole fraction, –	Ratio, –	Predicted mole fraction, –	Ratio, –	Predicted mole fraction, –	Ratio, –
Original	1.6E-03	1	2.3E-06	1	3.5E-07	1	5.1E-07	1	2.2E-09	1	1.6E-05	1
+Attempt 1	1.6E-03	1	1.3E-05	5	3.5E-07	1	5.0E-07	1	5.1E-09	2	1.9E-05	1
+Attempts 1 and 2	1.6E-03	1	1.3E-05	6	3.5E-07	1	5.1E-07	1	5.1E-09	2	2.0E-05	1
+Attempts 1, 2, and 3	2.0E-03	1	5.2E-05	22	3.3E-05	93	3.3E-05	65	1.0E-06	482	4.2E-05	3

Attempt 2

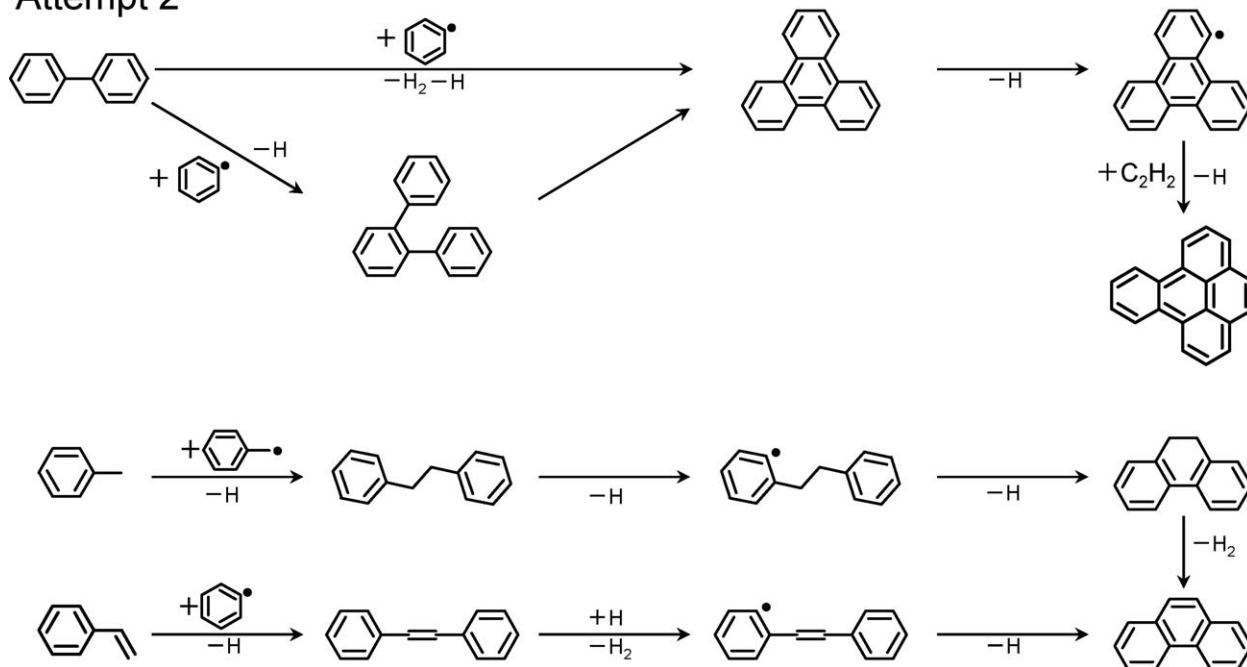


Fig. 4. Reaction schemes proposed in Attempt 2, including benzo[e]pyrene formation through terphenyl and triphenylene, and phenanthrene formation through diphenylethane, diphenylethylene, and diphenylacetylene.

5.3. Third attempt: reactions between cyclopentadienyl, indenyl, and benz[f]indenyl radicals

The last attempt was to include reactions between cyclopentadienyl, indenyl, and benz[f]indenyl radicals. The importance of resonance-stabilized radicals, such as cyclopentadienyl and indenyl radicals, was first identified by Marinov et al. [36], who investigated PAH formation in methane and ethylene flames through both experimental and detailed kinetic modeling studies. They found that acetylene addition processes were insufficient to account for the PAH levels observed in experimental flames. Inclusions of reactions such as naphthalene formation via cyclopentadienyl self-combination and phenanthrene formation from cyclopentadienyl and indenyl combination made their kinetic model precisely predictable. While these reactions were already

involved in our original mechanism [16], the formation of PAHs larger than phenanthrene was still significantly underestimated.

Lu and Mulholland [37] studied PAH growth from indene experimentally and observed three C₁₈H₁₂ isomers (chrysene, benz[a]anthracene, and benzo[c]phenanthrene) as the major products. They proposed reaction pathways leading to the C₁₈H₁₂ isomers by combination of indenyl radicals, as shown in Fig. 5. Based on the possible presence of benz[f]indene in the pyrolysis products, the reaction between benz[f]indene and cyclopentadiene was also considered. To produce benz[f]indene, a reaction between naphthyl 2-methyl radical and acetylene was proposed, analogous to indene formation by the reaction between benzyl radical and acetylene. A reaction between indenyl radical with acetylene to form naphthyl 2-methyl radical was also proposed, analogous to benzyl formation by the

Attempt 3

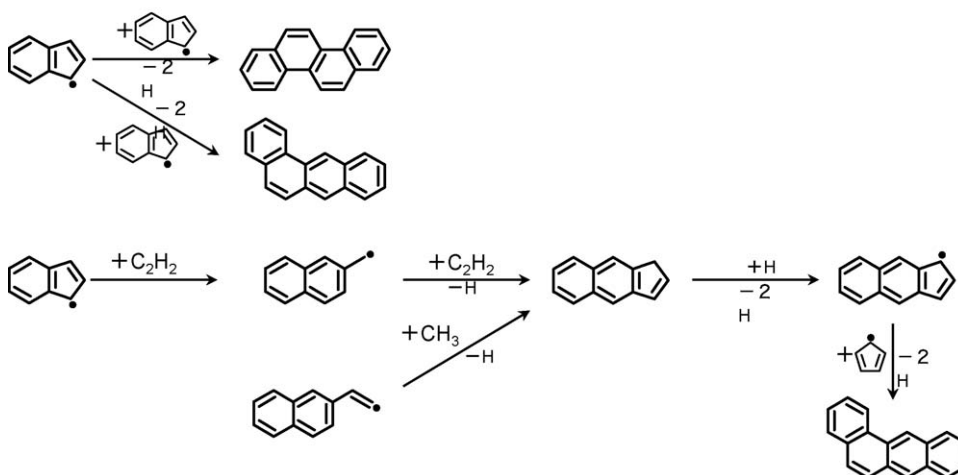


Fig. 5. Reaction schemes proposed in Attempt 3, including benzo[a]anthracene and chrysene formation by reactions between indenyls and through benzo[f]indene.

reaction between cyclopentadienyl radical and acetylene. The associated reactions are listed in Table 2. The rate constants for the reactions between cyclopentadienyl radicals to form naphthalene (No. 395) and between cyclopentadienyl and indenyl radicals to form phenanthrene (No. 557) were also changed from those used in the original mechanism [16]. The rate constants used for reaction Nos. 395 and 557 were those suggested originally by Marinov et al. [36]. The rate constants for the newly proposed reactions (Nos. 899, 900, and 908) were estimated at one-tenth of the rate constant for reaction No. 557. As shown in Table 3, the third attempt increased the predicted mole fractions of benz[a]anthracene, chrysene, and benzo[a]pyrene significantly, and the predicted values were comparable with the measured mole fractions.

Changes in enthalpy, entropy, and Gibbs free energy of the reaction sequences that were included in the Attempts 1, 2, and 3, were calculated based on the thermochemical parameters of the species involved in each reaction and are listed in the Supporting Information. The reaction sequences which are thermodynamically unfavorable (positive ΔG) are involved in the attempts, however this does not mean that these reactions are actually unrealistic. Because the equilibrium constants ranges between 0.98 and 1.00, indicating that the concentrations of the products are almost similar with those of reactants.

5.4. Predictive capabilities over the temperature range 1073–1373 K

Of the three attempts, the third had the most significant effect on improving the predictability of concentrations for benz[a]anthracene, chrysene, and benzo[a]pyrene, which were greatly underestimated by the original reaction mechanism [16]. Shown in Figs. 6

and 7 are comparisons between the numerical predictions by the modified mechanism and the measured mole fractions for typical PAHs at temperatures ranging from 1073 to 1373 K in the pyrolysis of propylene and acetylene, respectively. The predictions by the original mechanism [16] are also shown to highlight the improvement in predictive capabilities of the modified mechanism, which consists of 241 species and 902 reactions (*i.e.*, all reactions listed in Table 2) added to the original mechanism [16]. The complete set for the reaction mechanism, references of each of the elementary reactions, thermodynamic data for all species, and the species nomenclature are provided in the Supporting Information.

The original mechanism predicted the mole fraction profiles for phenanthrene and benzo[e]pyrene fairly well in the pyrolysis of both propylene and acetylene, whereas it significantly underestimated the mole fraction profiles for other PAHs. The deviations appeared to increase with decreasing temperature, while better agreements were obtained at temperatures above 1323 K. In the original mechanism [16], the PAH formation mechanism was acquired from the high-temperature flame-modeling study by Richter et al. [38], in which aryl–aryl combination and the HACA mechanism were the predominant reaction pathways for aromatic growth. Predictions by the original mechanism were highly temperature dependent. For instance, the predicted mole fraction of benz[a]anthracene in acetylene pyrolysis ranged from 10^{-8} to 10^{-4} for temperatures increasing from 1073 to 1373 K, whereas the measured mole fraction of benzo[a]pyrene ranges from 10^{-6} to 10^{-4} . A large underestimation, four orders in magnitude, was found at 1073 K. New reaction pathways for PAH formation other than aryl–aryl combination and the HACA mechanism are obviously necessary to fill in the gaps between the experimental data and numerical simulations, in particular at low temperatures.

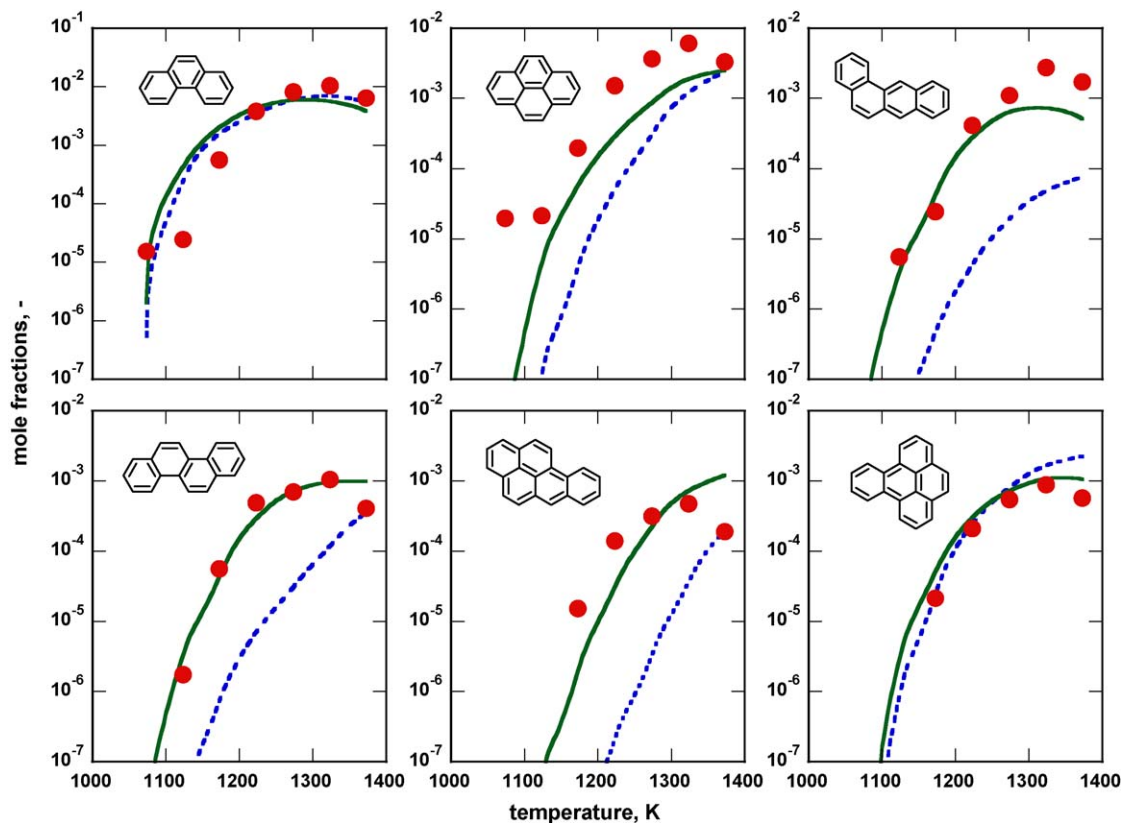


Fig. 6. Comparison of the computational predictions to the experimental data for typical PAHs (phenanthrene, pyrene, benzo[a]anthracene, chrysene, benzo[a]pyrene, and benzo[e]pyrene) found in the pyrolysis of propylene at 8 kPa and a residence time of 0.5 s as functions of the quasi-isothermal zone temperature. Lines and symbols represent the predictions and experimental data, respectively. Dashed lines represent the predictions provided by the mechanism of Ref. [16], while solid lines correspond to the predictions from the modified mechanism proposed in this study.

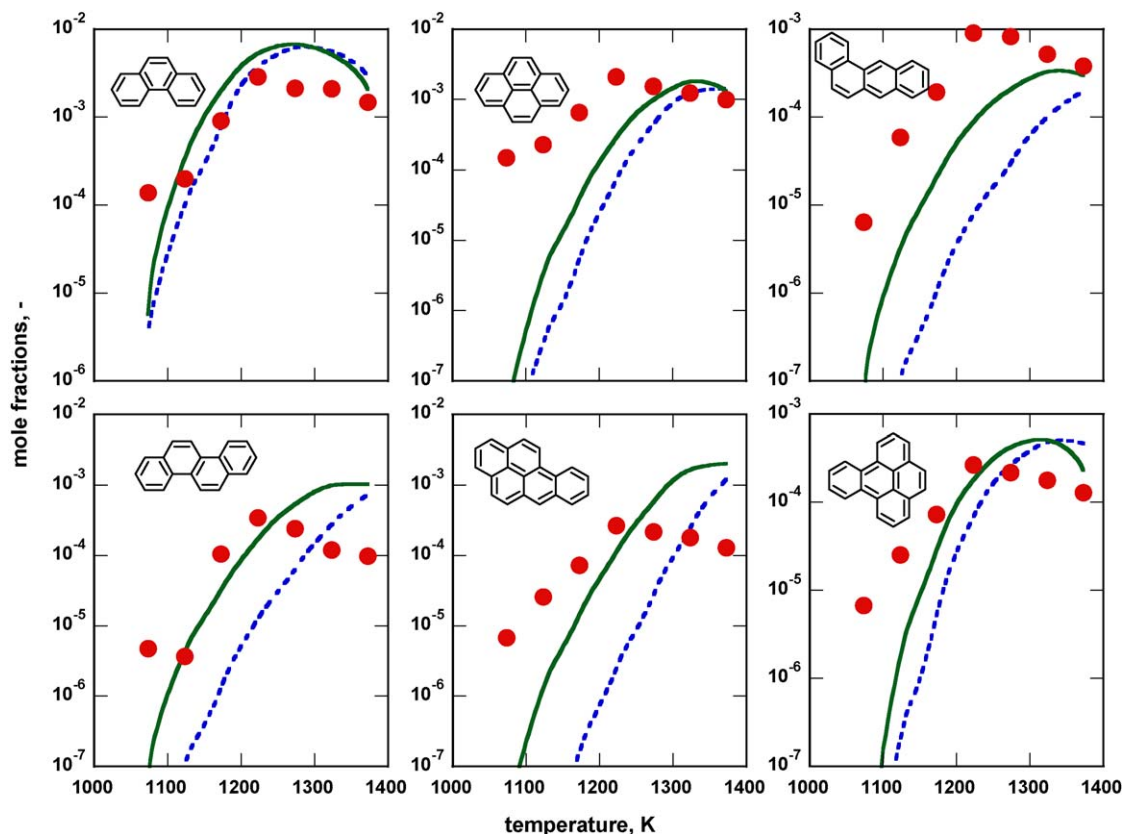


Fig. 7. Comparison of the computational predictions to the experimental data for typical PAHs (phenanthrene, pyrene, benzo [a]anthracene, chrysene, benzo[a]pyrene, and benzo[e]pyrene) found in the pyrolysis of acetylene at 8 kPa and a residence time of 0.5 s as functions of the quasi-isothermal zone temperature. Lines and symbols represent the predictions and the experimental data, respectively. Dashed lines correspond to the predictions provided by the mechanism of Ref. [16], while solid lines correspond to the predictions from the modified mechanism proposed in this study.

The third attempt increased the predicted mole fractions of PAHs such as benz[a]anthracene, chrysene, and benzo[a]pyrene most significantly at 1173 K (Table 3). The data shown in Figs. 6 and 7 demonstrate that such improvements may be achieved over the whole temperature range. Better agreement between the experiments and simulations were obtained, although underestimations of pyrene, benz[a]anthracene, benzo[a]pyrene, and benzo[e]pyrene at temperatures below 1223 K in the acetylene pyrolysis remained. In addition, undesired overestimations of benz[a]pyrene at temperatures above 1273 K in the pyrolysis of both propylene and acetylene were created upon modification of the original mechanism. Complete agreements are still challenging to accomplish, and clearly further efforts are required in both experiments and numerical simulation. It is safe to say, however, that the present modifications, especially the reaction schemes in the third attempt, which were not considered previously, are necessary to obtain better predictions of benz[a]anthracene, chrysene, and benzo[a]pyrene mole fraction profiles in the pyrolysis of light hydrocarbons at temperatures below 1300 K.

5.5. Influence of mechanism modification on predictability for major species

The current modifications succeeded in enhancing the predictive capabilities for PAH concentrations. The effect of the modifications on the mole fraction profiles of major species is illustrated in Fig. 8, where computational predictions are compared with the experimental data for major compounds (mole fractions $>10^{-3}$) found in the propylene pyrolysis as functions of the quasi-isothermal zone temperature. The computed mole

fractions were hardly influenced by the modifications, and the updated mechanism gave predictions similar those from the original mechanism for the major species [21]. Similar results were also obtained using the data for ethylene and acetylene pyrolysis. Although the modifications induced increases in the predicted mole fractions by one to four orders of magnitude, the PAHs were still minor components with mole fractions ranging from 10^{-6} to 10^{-3} , and thereby had a negligible influence on the prediction of major species.

5.6. Formation pathways leading to two of the largest PAHs, coronene and anthanthracene, in acetylene pyrolysis

A reaction flux analysis using the modified mechanism was performed to identify the chemical pathways believed to be important for aromatic and PAH growth. Shown in Fig. 9 is a reaction flux diagram for the important pathways leading to the formation of two of the largest PAHs, coronene and anthanthracene, in acetylene pyrolysis at 1173 K, 8 kPa, and a residence time of 0.5 s. The arrows represent the formation flow of each species. The contribution of a reaction to the formation of a species is expressed by the arrow thickness, which was graded into six different levels.

Coronene is formed exclusively from a reaction of acetylene addition to benz[ghi]perylene radical. There are two precursor PAHs of benz[ghi]perylene: perylene and benz[e]pyrene. The former is generated almost exclusively by a reaction between 1-naphthyl radical and naphthalene, while the latter is formed almost exclusively by a reaction between phenyl radical and phenanthrene. Naphthalene is formed primarily by a decomposition of

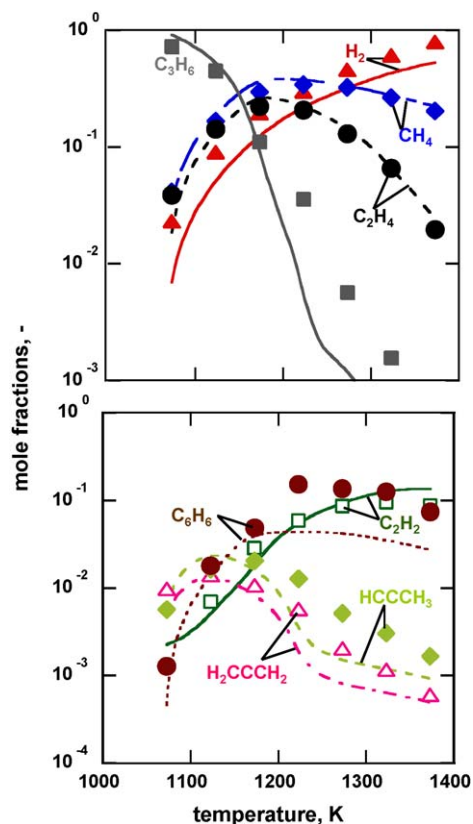


Fig. 8. Comparison of the computational predictions to the experimental data for major species found in the pyrolysis of propylene at 8 kPa and a residence time of 0.5 s as functions of the quasi-isothermal zone temperature. Lines and symbols represent the predictions obtained from the modified mechanism proposed in this study and the experimental data, respectively.

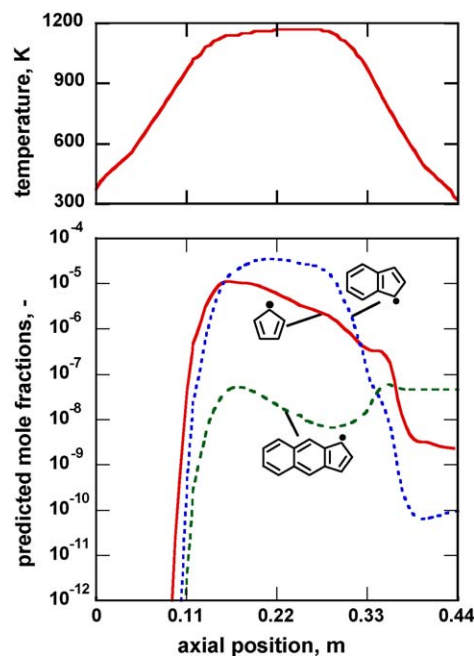


Fig. 10. The reactor wall temperature and predicted mole fractions of cyclopentadienyl, indenyl, and benz[f]indenyl radicals as a function of reactor axial position in the pyrolysis of acetylene at 8 kPa, 1173 K (quasi-isothermal zone), and a residence time of 0.5 s.

2-methylnaphthalene, and secondarily by a reaction between vinylacetylene and phenyl radical. Phenanthrene is formed mainly by a phenyl radical addition to phenylacetylene. A reaction between cyclopentadienyl and indenyl radicals contributes 7% to phenanthrene formation.

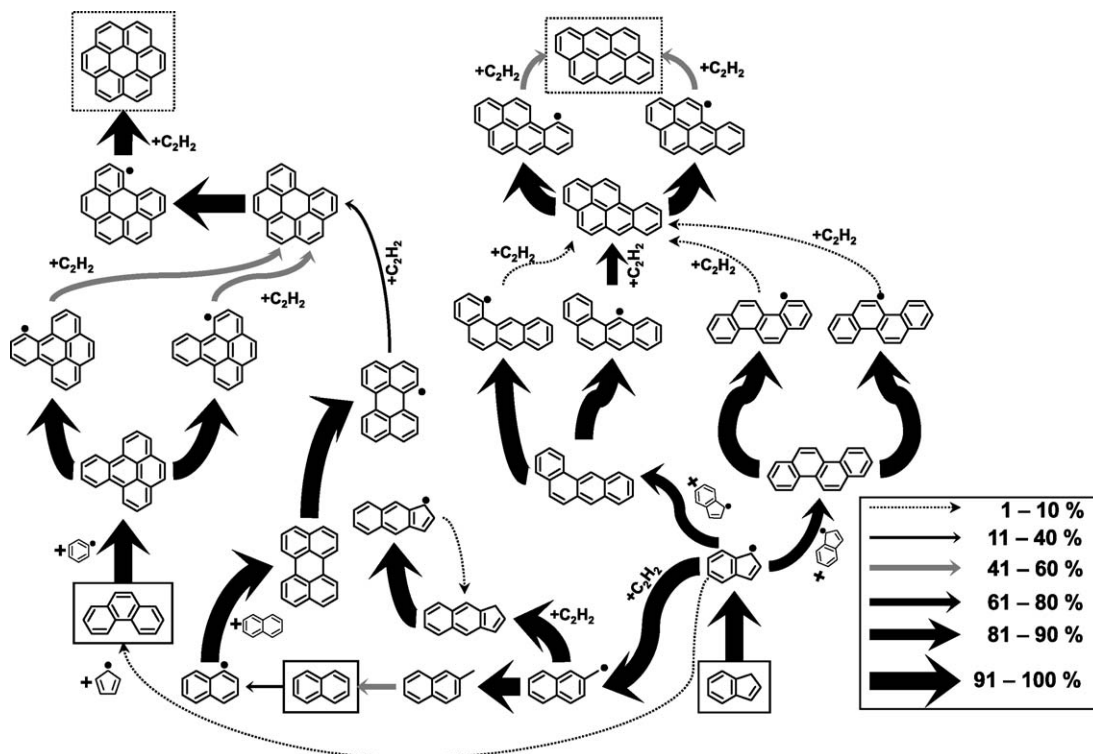


Fig. 9. Reaction flux diagram for PAH formation in acetylene pyrolysis at 1173 K, 8 kPa, and a residence time of 0.5 s.

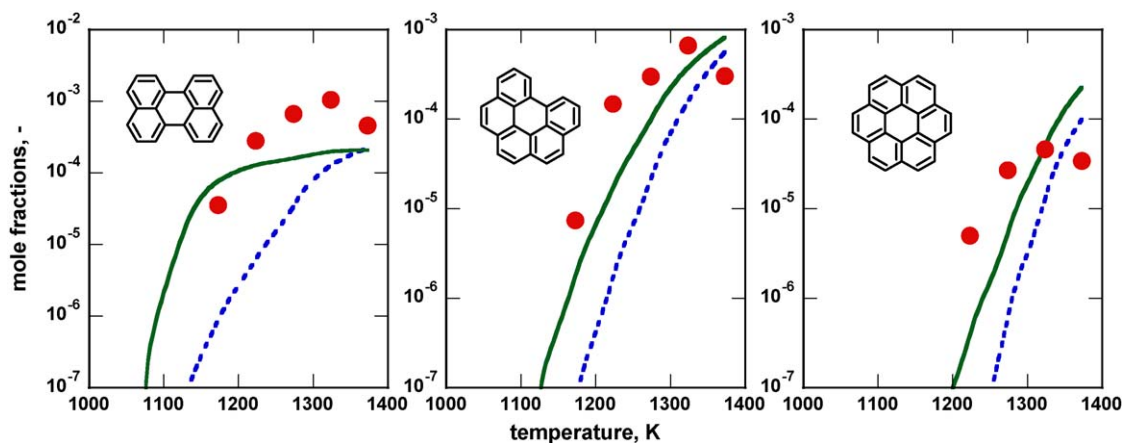


Fig. 11. Comparison of the computational predictions to the experimental data for typical PAHs (perylene, benzo[ghi]perylene, and coronene) found in the pyrolysis of propylene at 8 kPa and a residence time of 0.5 s as functions of the quasi-isothermal zone temperature. Lines and symbols represent the predictions and the experimental data, respectively. Dashed lines correspond to the predictions provided by the mechanism of Ref. [16], while solid lines correspond to predictions from the modified mechanism proposed in this study.

Anthracene is produced by acetylene additions to two types of benz[a]pyrene radicals. There are two pathways leading to benz[a]pyrene that go through benzo[a]anthracene and chrysene. The contributions to benz[a]pyrene formation by benzo[a]anthracene radical and chrysene radical are 90% and 8%, respectively; indicating that benzo[a]anthracene radical is the dominant precursor. The 90% is formed by the self-combination of indenyl radicals—reactions necessary for improving the predictability of the selected PAHs, as demonstrated in Figs. 6 and 7. In the original mechanism, a reaction between phenylethynyl radical and naphthalene was a major route to benz[a]anthracene and chrysene. This was, however, insufficient to produce results comparable to the measured concentrations. Their contributions were only 4% using the modified mechanism.

A reaction between benz[f]indenyl and cyclopentadienyl radicals (No. 901, Table 2) was also proposed as a new route to benzo[a]anthracene, but its contribution to benzo[a]anthracene formation was negligible. Depicted in Fig. 10 are the reactor wall temperature and predicted mole fractions of cyclopentadienyl, indenyl, and benz[f]indenyl radicals as functions of the reactor axial position in the acetylene pyrolysis at 1173 K. The predicted concentrations in the quasi-isothermal zone for cyclopentadienyl and indenyl radicals were about 10^{-5} to 10^{-6} , whereas, that for benz[f]indenyl radical was approximately 10^{-8} . As listed in Table 2, the rate constant for the self-combination of indenyl radicals (No. 894) is same as that for reaction 901. Based on the reactant concentrations and the rate constant, it is suggested that the rate of formation for benz[a]anthracene via reaction 894 is greater than that via reaction 901 by three to four orders of

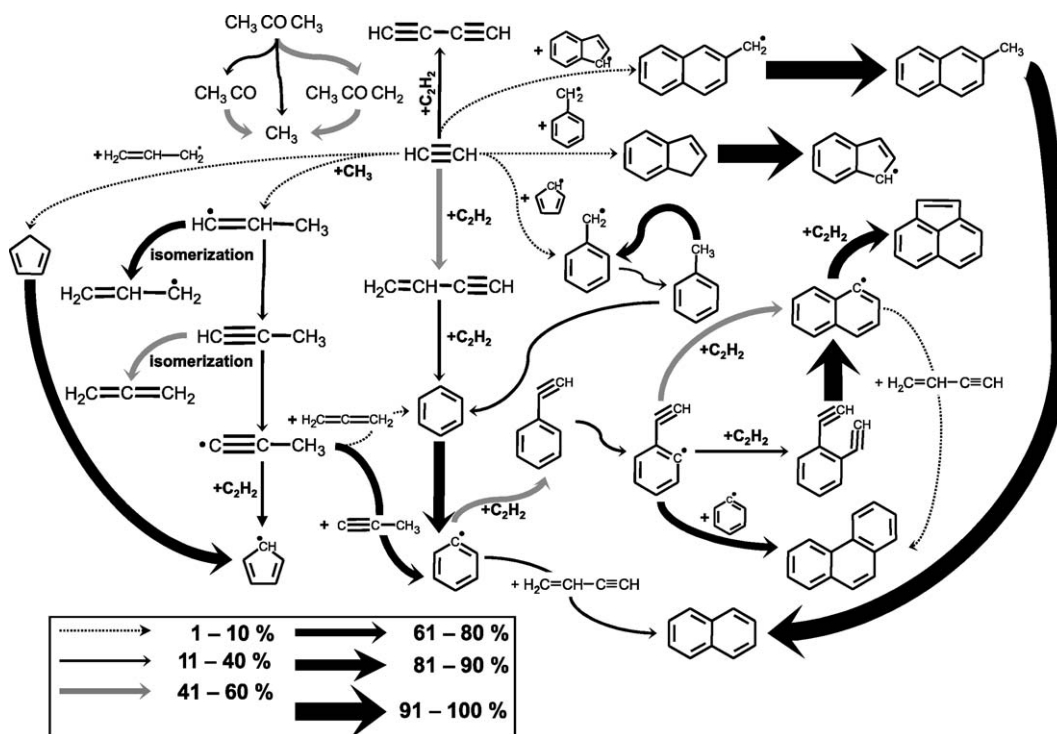


Fig. 12. Reaction flux diagram for the consumption of acetylene leading to important aromatic hydrocarbon formations in acetylene pyrolysis at 1173 K, 8 kPa, and a residence time of 0.5 s.

magnitude, making it almost negligible for benzo[a]anthracene formation.

The inclusion of benz[f]indene in the PAH growth had little effect on the predictions. However, it would make sense to add a reaction to form naphthyl 2-methyl radical, which converts to 2-methylnaphthalene and further to naphthalene, because the predictive capabilities of perylene, benz[ghi]perylene, and coronene are also improved, as shown in Fig. 11. Since the indenyl radical self-combination reaction should have no effect on the formation of these PAHs, the improvements are likely brought by the enhanced production of naphthalene.

The formation pathway analysis for coronene and anthanthracene indicated that these PAHs were formed from distinctly different precursor aromatics. Similar results were also obtained for ethylene and propylene pyrolysis. Coronene originates from naphthalene and phenanthrene, whereas anthanthracene comes from indene. This means that the composition of the large PAHs is controlled strongly by the presence as well as the population of these aromatics. The following results from the consumption flow analysis are presented to identify how these important aromatics are formed from the precursor hydrocarbons. While the reaction pathway analyses from the precursor hydrocarbons to benzene for ethylene, acetylene, and propylene pyrolyses were reported previously [16,21], an extended analysis was performed here. Particular attention was paid to the role of acetone in the formation of the important PAHs in the acetylene pyrolysis to investigate the underestimations of large PAHs, which were still observed at low temperatures.

5.7. Consumption pathways leading to important precursors for PAHs in acetylene pyrolysis

Shown in Fig. 12 is a reaction flux diagram for the acetylene pyrolysis based on a rate-of-consumption analysis at 1173 K, 8 kPa, and a residence time of 0.5 s. The contribution of a reaction to the consumption of a species is expressed by the arrow thickness, which was graded into six different levels.

Acetylene is consumed primarily by dimerization to form vinylacetylene, and secondarily by dimerization to form diacetylene. Besides these self-combinations, acetylene pyrolysis is also initiated by reaction with radicals such as methyl, allyl, cyclopentadienyl, benzyl, and indenyl radicals. Acetylene reacts with methyl radical to form 2-methylvinyl radical, which further converts primarily into allyl radical by isomerization and secondarily into propyne. Acetylene reacts with thus formed allyl radical to form cyclopentadiene, which further converts into cyclopentadienyl radical. The reaction between acetylene and cyclopentadienyl radical produces benzyl radical. Acetylene reacts with benzyl radical to form indene, which further converts into indenyl radical. It is clear that methyl radical is an initiator for the formation of important radicals such as cyclopentadienyl and indenyl radicals that are necessary for PAH growth. However, methyl radical is not produced directly from acetylene but from acetone. The acetone consumption flux is also given in Fig. 12. The rate-of-formation analysis for methyl radical at conditions similar to those in Fig. 12 indicated that nearly 90% of methyl originated from acetone.

Numerical simulations were conducted to study the influence of acetone concentration in the gas inlet on the predicted concentrations of PAHs. Fig. 13 compares the numerical predictions with the measured mole fractions for benzo[a]anthracene and benzo[a]pyrene in the pyrolysis of acetylene. The predicted mole fractions of both benzo[a]anthracene and benzo[a]pyrene increased with increasing acetone concentration, approaching the measured values. The acetone concentration was a function of the gas cylinder pressure and temperature. Bergmann et al. [26] calculated that the acetone concentration changes from approximately 0.5% in full gas cylinders

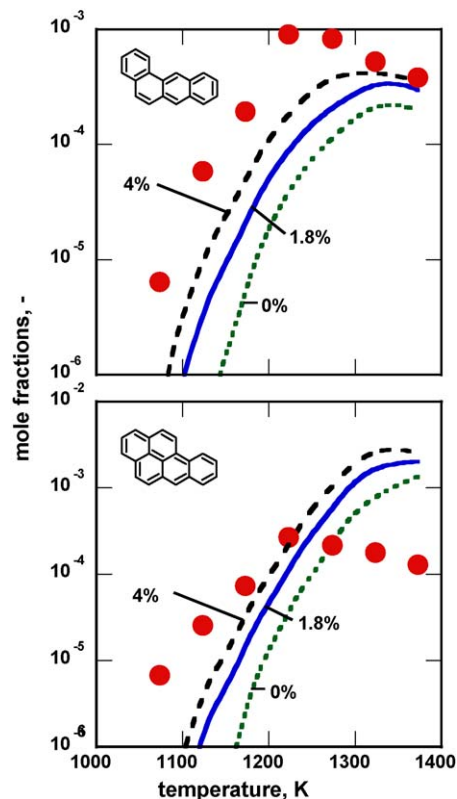


Fig. 13. Influence of acetone concentration in the gas inlet on the computational predictions for benzo[a]anthracene and benzo[a]pyrene in the pyrolysis of acetylene at 8 kPa and a residence time of 0.5 s as functions of the quasi-isothermal zone temperature. Lines and symbols represent the predictions obtained using the modified mechanism proposed in this study and the experimental data, respectively. Values are acetone mol% in the gas inlet.

to more than 10% in nearly empty ones. The acetone concentration should be different in each test of our study. The uncertainty of the acetone concentration in the gas inlet is likely one cause of the gap that remains between the experimental data and the predicted values in the PAH profiles in acetylene pyrolysis, even when the present modified mechanism was applied.

6. Summary

The motivation for this study was to fill in the gaps between experimental determination and numerical simulation of the concentration profiles for large PAHs produced in the pyrolyses of unsaturated light hydrocarbons using a detailed chemical kinetic model.

Three attempts were made to improve the model capabilities for predicting PAH concentrations. The first attempt involved the addition of reaction schemes for enhancing PAH radical generations by attack of methyl and vinyl radicals. The second attempt included reaction schemes for phenanthrene formation through 1,2-diphenylethylene and 1,2-diphenylacetylene, and benz[e]pyrene formation through triphenylene. These were proposed based on a detailed analysis of pyrolysates with GC/MS. The third attempt involved reactions between cyclopentadienyl, indenyl, and benz[f]indenyl radicals to form benzo[a]anthracene and chrysene, which were underestimated by one to four orders of magnitude in the previous kinetic model [16].

Comparisons between numerical simulations using the detailed chemical reaction schemes coupled with a plug flow reactor model and experimental data for a flow reactor at 1073–1373 K revealed that the third attempt had the most significant effect on improving

the model performance, whereas the first and second attempts only exhibited small improvements. The modified mechanism, consisting of 241 species and 902 reactions, can account for the formation of large PAHs such as benz[a]anthracene, chrysene, and benz[a]pyrene almost perfectly for propylene pyrolysis. Critical evaluation of this channel will occur when the required rate constants are established with higher confidence.

The modified mechanism, however, is not sufficient to account for the formation of large PAHs in acetylene pyrolysis. A reaction flux analysis for acetylene pyrolysis revealed the important role of acetone as a source of methyl radical, which enhances the formation of cyclopentadienyl and indenyl radicals. The predicted mole fractions of both benz[a]anthracene, chrysene, and benz[a]pyrene increased with increasing acetone concentration and approach the measured values. The uncertainty of the acetone concentration in the gas inlet is likely to be one cause of the gap that remains between the experimental data and the predicted values for the PAH profiles for the acetylene pyrolysis, even when the present modified mechanism is applied.

Nevertheless, before details of the pyrolysis of light hydrocarbons, as well as the formation pathways of PAHs, may be predicted satisfactorily, more detailed studies on gas-phase chemistry, surface (deposition) chemistry, and transport models such as molecular diffusion of species in both the axial and radial directions are required.

Acknowledgements

Part of this research, performed in the Sonderforschungsbereich (SFB) 551 “Carbon from gas-phase: elementary reactions, structures, materials,” was funded by the Deutsche Forschungsgemeinschaft (DFG). The authors acknowledge the use of the computer program HOMREA by Prof. J. Warnatz (University of Heidelberg). K.N. also acknowledges support from the Ministry of Education, Science, Sports and Culture Grant-in-Aid for Young Scientists (No. 20760518).

Appendix A. Supplementary data

Supplementary data associated with this article can be found, in the online version, at doi:10.1016/j.jaap.2009.05.001.

References

- [1] A. Oberlin, Carbon 40 (2002) 7–24.
- [2] S. Bammidipati, G.D. Stewart, J.R. Elliott, S.A. Gokoglu, M.J. Purdy, AIChE J. 142 (1996) 3123–3132.
- [3] A. Becker, Z. Hu, K.J. Hüttinger, J. Phys. IV 9 (1999) 41–47.
- [4] V. De Pauw, B. Reznik, S. Kalhofer, D. Gerthsen, Z.J. Hu, K.J. Hüttinger, Carbon 41 (2003) 71–77.
- [5] O. Feron, F. Langlais, R. Naslain, Chem. Vapor Depos. 5 (1999) 37–47.
- [6] O. Feron, F. Langlais, R. Naslain, J. Thebault, Carbon 37 (1999) 1343–1353.
- [7] I. Ziegler, R. Fournet, P.M. Marquaire, J. Anal. Appl. Pyrol. 73 (2005) 107–115.
- [8] S. Vaidyaraman, W.J. Lackey, P.K. Agrawal, M.A. Miller, Carbon 34 (1996) 347–362.
- [9] A. Becker, K.J. Hüttinger, Carbon 36 (1998) 201–211.
- [10] A. Becker, K.J. Hüttinger, Carbon 36 (1998) 177–199.
- [11] K. Norinaga, K.J. Hüttinger, Carbon 41 (2003) 1509–1514.
- [12] M. Kawase, K. Miura, Thin Solid Films 498 (2006) 25–29.
- [13] L.F. Albright, J.C. Marek, Ind. Eng. Chem. Res. 27 (1988) 743–751.
- [14] K.J. Hüttinger, Chem. Vapor Depos. 4 (1998) 151–158.
- [15] A.M. Dean, J. Phys. Chem. 94 (1990) 1432–1439.
- [16] K. Norinaga, O. Deutschmann, Ind. Eng. Chem. Res. 46 (2007) 3547–3557.
- [17] C. Descamps, G.L. Vignoles, O. Feron, F. Langlais, J. Lavenac, J. Electrochem. Soc. 148 (2001) C695–C708.
- [18] I. Ziegler, R. Fournet, P.M. Marquaire, J. Anal. Appl. Pyrol. 73 (2005) 212–230.
- [19] I. Ziegler, R. Fournet, P.M. Marquaire, J. Anal. Appl. Pyrol. 73 (2005) 231–247.
- [20] C.Y. Sheng, A.M. Dean, J. Phys. Chem. A 108 (2004) 3772–3783.
- [21] K. Norinaga, V.M. Janardhanan, O. Deutschmann, Int. J. Chem. Kinet. 40 (2008) 199–208.
- [22] K. Norinaga, O. Deutschmann, K.J. Hüttinger, Carbon 44 (2006) 1790–1800.
- [23] G.L. Dong, K.J. Hüttinger, Carbon 40 (2002) 2515–2528.
- [24] M.J. Wornat, C.J. Mikolajczak, B.A. Vernaglia, M.A. Kalish, Energy Fuels 13 (1999) 1092–1096.
- [25] M.J. Wornat, E.B. Ledesma, N.D. Marsh, Fuel 80 (2001) 1711–1726.
- [26] U. Bergmann, K. Lummer, B. Atakan, K. Kohse-Hoinghaus, Berichte Der Bunsen-Gesellschaft-Phys. Chem. Chem. Phys. 102 (1998) 906–914.
- [27] J. Warnatz, U. Maas, R.W. Dibble, Combustion, 3rd Edition, Springer-Verlag, Heidelberg, New York, 2000.
- [28] H. Wang, M. Frenklach, J. Phys. Chem. 98 (1994) 11465–11489.
- [29] H. Wang, M. Frenklach, Combust. Flame 110 (1997) 173–221.
- [30] O.S.L. Bruinsma, J.A. Moulijn, Fuel Process. Technol. 18 (1988) 213–236.
- [31] S.W. Benson, Methods for the Estimation of Thermochemical Data and Rate Parameters, Wiley, New York, 1976.
- [32] W.H. Green, P.I. Barton, B. Bhattacharjee, D.M. Matheu, D.A. Schwer, J. Song, R. Sumathi, H.H. Carstensen, A.M. Dean, J.M. Grenda, Ind. Eng. Chem. Res. 40 (2001) 5362–5370.
- [33] J. Song, S. Raman, J. Yu, C.D. Wijaya, G. Stephanopoulos, W.H. Green, Abstr. Pap. Am. Chem. Soc. 226 (2003) U530–U531.
- [34] J. Song, R. Sumathi, J. Yu, W.H. Green, Abstr. Pap. Am. Chem. Soc. 228 (2004) U233–U233.
- [35] K.M. Van Geem, M.F. Reyniers, G.B. Marin, J. Song, W.H. Green, D.M. Matheu, AIChE J. 52 (2006) 718–730.
- [36] N.M. Marinov, W.J. Pitz, C.K. Westbrook, M.J. Castaldi, S.M. Senkan, Combust. Sci. Technol. 116 (1996) 211–287.
- [37] M.M. Lu, J.A. Mulholland, Chemosphere 42 (2001) 625–633.
- [38] H. Richter, J.B. Howard, Phys. Chem. Chem. Phys. 4 (2002) 2038–2055.